Available online at www.sciencedirect.com
SCIENCE DIRECT
Catalysis Today 107–108 (2005) 149–156
CATALYSIS TODAY
www.elsevier.com/locate/cattod

SCR of NO by CH_4 on Pt/ZrO_2–TiO_2 sol–gel catalysts

R. Pérez-Hernández [a,b], A. Gómez-Cortés [c], J. Arenas-Alatorre [c], S. Rojas [d], R. Mariscal [d], J.L.G. Fierro [d], G. Díaz [c,*]

[a] *ININ, Km. 36.5, Carr. México–Toluca Salazar, C.P. 52045, Edo. De México, México*
[b] *FQ-UAEM, C.P. 50120, Toluca, México*
[c] *Instituto de Física-UNAM, Apdo. Postal 20-364, C.P. 01000, México D.F., México*
[d] *ICP-CSIC, Cantoblanco, 28049 Madrid, Spain*

Available online 15 August 2005

Abstract

ZrO_2–TiO_2 mixed oxides with various $ZrO_2/ZrO_2 + TiO_2$ composition (0.9, 0.5 and 0.1) were prepared by the sol–gel method and used as catalytic support for Pt. As a function of the support composition the surface area of ZrO_2–TiO_2 oxides goes through a maximum (552 m^2/g) for the (ZT0.5) support whose surface area was almost nine times higher than that of the single oxides (around 60 m^2/g). Also, different reducibility properties of the platinum oxide were observed. The catalytic performance of the solids was studied using the selective reduction of NO with CH_4. The steady-state activity of the catalysts was also dependent on the support composition. The reactivity of the catalysts (TON) in the range 573–773 K follows the order: $Pt/ZT(0.9) > Pt/ZrO_2 \approx Pt/ZT(0.5) \approx Pt/ZT(0.1) > Pt/TiO_2$. The Pt/ZT(0.9) catalyst which includes in the support formulation 10 mol% of TiO_2 showed the highest catalytic activity with TON values 2.5 times higher than those found in Pt/ZrO_2. Also the selectivity for N_2 production was slightly higher for this catalyst. The addition of N_2O as an oxygen source for NO oxidation was also evaluated. All catalysts improved their performance in the presence of N_2O. The combination of acid properties, particle size and the presence of stable isocyano type intermediates which characterize the Pt/ZT(0.9) catalyst could explain its performance.

Keywords: Pt/ZrO_2–TiO_2; SCR; NO + CH_4; Characterization; Sol–gel

1. Introduction

The removal of NO_x from exhaust gases is still one of the greatest challenges in the field of Environment Protection. Various approaches have been taken depending on the application, and the selective reduction with ammonia is one of the most commonly used technologies [1]. The selective catalytic reduction of nitric oxide with hydrocarbons (HC-SCR) has received increased attention in the last years and this is due to the need for replacing the NH_3-SCR process. Among hydrocarbons, methane offers the benefits of low cost and wide availability compared to other hydrocarbons. Its relative inertness provides however lower activity than other reduction gases over most catalytic systems [2,3]. Therefore, efforts have been focused on the development of CH_4-SCR catalysts that will be active, selective and stable. It has been recognised that strong acidic catalysts are the most active for HC-SCR reaction and these include strongly acidic zeolites [4–6], sulphated zirconia or binary oxides [7]. Mixed oxides have been used as support for HC-SCR catalyst. Hosose et al. [8] reported that the addition of copper to SiO_2–Al_2O_3 binary oxides enhanced the catalytic activity for NO reduction by ethane. On the other hand, Haneda et al. [9] reported that silver supported TiO_2–ZrO_2 catalyst showed high activity for NO reduction by propene in presence of oxygen and confirmed that TiO_2–ZrO_2 binary oxide can be used as a good catalytic support for this reaction. Mixed ZrO_2–TiO_2 oxide display some interesting features as the presence of both acidic and basic sites, high BET surface area and high thermal resistance with respect to its individual ZrO_2 and TiO_2 components [10]. Moreover, it has been reported [11] that addition of ZrO_2 to TiO_2 may prevent the migration of reduced TiO_x moieties onto the

* Corresponding author. Tel.: +52 55 56225097; fax: +52 55 56225008.
E-mail address: diaz@fisica.unam.mx (G. Díaz).

0920-5861/$ – see front matter
doi:10.1016/j.cattod.2005.07.080

metal particles after high temperature reduction and by this the strong metal–support interaction (SMSI) may be inhibited.

The aim of this work is to investigate the properties of Pt supported on mixed ZrO_2–TiO_2 oxides of various compositions as catalyst for the NO reduction by CH_4 reaction. The support ZrO_2–TiO_2 with different molar ZrO_2/TiO_2 ratios was synthesised by the sol–gel method and a detailed characterization of physical and chemical properties of the solids was achieved. The evolution of the xerogels as a function of temperature was followed by TG/DSC analysis. Textural and structural properties were characterized by N_2 adsorption and DRX, respectively. TPR experiments were done to know about the reduction properties of the solids and Pt particle size and dispersion were evaluated from H_2 chemisorption measurements. The steady-state activity of the catalysts for the NO + CH_4 reaction was studied in a flow reactor under various reaction conditions. In a previous work [12] investigation of the surface properties of these catalysts was performed using XPS and DRIFT spectroscopy.

2. Experimental methods

2.1. Catalyst preparation

ZrO_2, TiO_2 and mixed ZrO_2–TiO_2 oxides were prepared by the sol–gel method using alcoxide precursors from Aldrich. For the preparation of ZrO_2 and TiO_2 oxides, the precursors, $Zr(OCH_2CH_2CH_3)_4$ (zirconium(IV) propoxide) and $Ti(OCH_2CH_2CH_3)_4$ (titanium(IV) propoxide), were first partially hydrolyzed at 291 K. For this purpose, the proper amount of the alcoxide was dissolved in $CH_3CH_2CH_2OH$ (*n*-propanol, Merck) and stirred vigorously until solution became homogeneous. Then, NH_4OH (Merck) was added and the solution was stirred for 5 more minutes (pH = 9). At this stage, the molar ratio, alcoxide/C_3H_7OH/H_2O/NH_4OH was 1/4/1/0.33. Temperature was then increased and after 10 min at reflux temperature, deionized water was added drop by drop to complete hydrolysis and reflux was continued for 1 h. The resultant mixture was cooled to room temperature. The gels were aged in situ for 24 h and the residual liquid was removed by decanting.

The same general protocol was used to prepare the ZrO_2–TiO_2 oxides. In this case, the proper amount of each alcoxide precursor to get the desired $ZrO_2/ZrO_2 + TiO_2$ molar ratio was used. In the first step of the synthesis the alcoxide of the main oxide in the formulation was partially hydrolyzed as described above. Afterwards, the second alcoxide was added. At this point temperature was increased to reach reflux temperature and hydrolysis was completed. In the case of the equimolar composition ($ZrO_2/ZrO_2 + TiO_2 = 0.5$) a mixture of the alcoxide precursors was used as starting material. Xerogels obtained after heating in an oven at 373 K for 24 h were calcined in static air using a temperature ramp of 5°/min. At first the samples were maintained for 1 h at 373 K and after this stage temperature was raised to 773 K and kept for 5 h.

Platinum (around 1 wt.%) was incorporated on the supports by classical impregnation using an aqueous solution of H_2PtCl_6 (Aldrich). After drying, the samples were calcined in air (60 cm^3/min) at 773 K for 2 h and then reduced in flowing H_2 (60 cm^3/min) at the same temperature for 1 h. The actual platinum content was determined by Energy Dispersive Spectroscopy (EDS) in a Philips XL-30 Scanning Electron Microscopy. In what follows, catalysts will be identified as follows: Pt/ZrO_2 and Pt/TiO_2 for Pt supported on the single oxides, and Pt/ZT(*M*) for Pt supported on ZT = ZrO_2–TiO_2 oxides and *M* = $ZrO_2/ZrO_2 + TiO_2$ molar ratio = 0.9, 0.5 and 0.1.

2.2. Characterization

The TG/DSC analysis of xerogels was carried out in a TGA-51 Thermogravimetric Analysis system and DSC-10 Differential Scanning Calorimeter (TA Instruments) under N_2 atmosphere in the range of 293–1073 K for TGA analysis and 293–873 K for DSC analysis at a heating rate of 10 K/min.

The specific surface area of the samples was determined by the BET method from N_2 adsorption (30% N_2/He gas mixture) using the single point method in a RIG-100 multitask characterization unit from ISRI. Samples were first degassed at 423 K for 1.5 h to eliminate moisture.

The crystallographic phase identification was performed by X-ray diffraction (XRD) in a Bruker Advance D-8 equipment with Cu Kα radiation and a graphitic secondary beam monochromator. Data were obtained in the 2θ range between 20° and 110° with a step of 0.02° and a measuring time of 2.7 s per point. The crystalline structures were refined using the Rietveld technique by means of Fullprof-V3.5D code [13].

TPR experiments were done using a characterization unit RIG-100 from In Situ Research Inc. For TPR runs, the sample (0.1 g) was placed in the reactor and purged with Ar at room temperature and then heated at a rate of 10 K/min in presence of a 5% H_2/Ar gas mixture (30 cm^3/min).

Pt particle size and dispersion were determined from chemisorption measurements in a volumetric system. Samples reduced at 773 K were reactivated in H_2 for 1 h at 673 K (for Ti-rich samples reduction and reactivation temperature was 573 K in order to avoid SMSI effects). After evacuation and cooling to 298 K, H_2 uptakes were measured. Total and irreversible adsorption isotherms were recorded.

2.3. Catalytic activity measurements

The steady-state reaction experiments were performed using a fixed-bed flow reactor on line with a GC (Gow Mac 580) for product analysis. The composition of the feed was 2500 ppm NO and 5250 ppm CH_4 in balance He at a

GHSV = 30500 h^{-1}. For experiments in presence of N_2O as a source of oxygen, 2500 ppm of N_2O was added to the feed. Prior to reaction, catalyst was reactivated in situ at 673 K in H_2 flow (60 cm^3/min) for 1 h. After this step the system was purged with He for 1 h and the temperature was set to initiate a run. To determine the activity of the catalyst as a function of the temperature, conversion of NO and CH_4 was followed in the 573–773 K range. For each reaction temperature activity was allowed to stabilize before temperature was increased. The reaction products were separated using two columns (4 m packed Carbosphere and Molecular Sieve 5A) at 358 K. Activity versus time on stream (24 h) experiment was performed at 673 K to study the stability of the catalysts. Total activity was followed by the NO conversion as a function of the reaction temperature and turn over number (TON) values were evaluated from chemisorption data and a steady-state NO reduction rate calculated as $-r_{NO} = \alpha F/\omega$, where, α is the NO conversion, F the flow rate of NO (mol/s) and ω is the weight of the catalyst (g).

3. Results and discussion

3.1. Thermal analysis

The TG curves of the xerogels are shown in Fig. 1a. Several components, such as physically adsorbed water, physically and chemically adsorbed alcohol and residual organic material coming from the synthesis may be removed and assigned to different steps in the TG curve. Sharp weight losses are observed in two temperature ranges, the first between 320 and 473 K and the second between 523 and 873 K. In general weight loss of the samples was around 30%. Related to this behavior, the DSC curves of all samples, Fig. 1b, present an endothermic peak in the first temperature range, which corresponds to elimination of physically adsorbed water and alcohol [14,15]. In the second temperature range, endothermic and exothermic processes take place. Dehydroxilation occurs between 573 and 673 K while exothermic peaks around 648–803 K are assigned to elimination and burning of organic residual material and crystallization processes of the oxides. Crystallization processes of ZrO_2 and TiO_2 are characterized by exothermic peaks in the range 673–723 K. The amorphous to anatase transformation of TiO_2 is reported to occur in the 673–753 K range [16] while the crystallization of tetragonal zirconia is reported around 700 K [17,15]. No exothermic peaks related to crystallization processes of the material were observed in the ZrO_2–TiO_2 sample with an equimolar composition (ZT0.5) in this temperature range although crystallization in a $ZrTiO_4$ phase is reported to occur around 900 K [17].

3.2. Textural properties

The BET surface area of the solids is presented in Table 1. The surface area of the ZrO_2–TiO_2 oxides goes through a maximum (552 m^2/g) for the (ZT0.5) support whose surface area was almost nine-fold higher than the one of the single oxides (around 60 m^2/g). When Pt is incorporated to the support the surface area decreases. This can be attributed to a blockage of the pores of the support by supported Pt particles. Nevertheless, as before, the same trend in the behavior of the surface area is observed as a function of the TiO_2 content in the support. The morphology of the supports may be observed in typical SEM images (Fig. 2). Grain size evolution is related to the TiO_2 content in the support. The Zr-rich supports present smaller grain size compared to Ti-rich samples. When the support composition is 1:1 grain size is intermediate between the grain size of the ZrO_2 and the TiO_2 oxides.

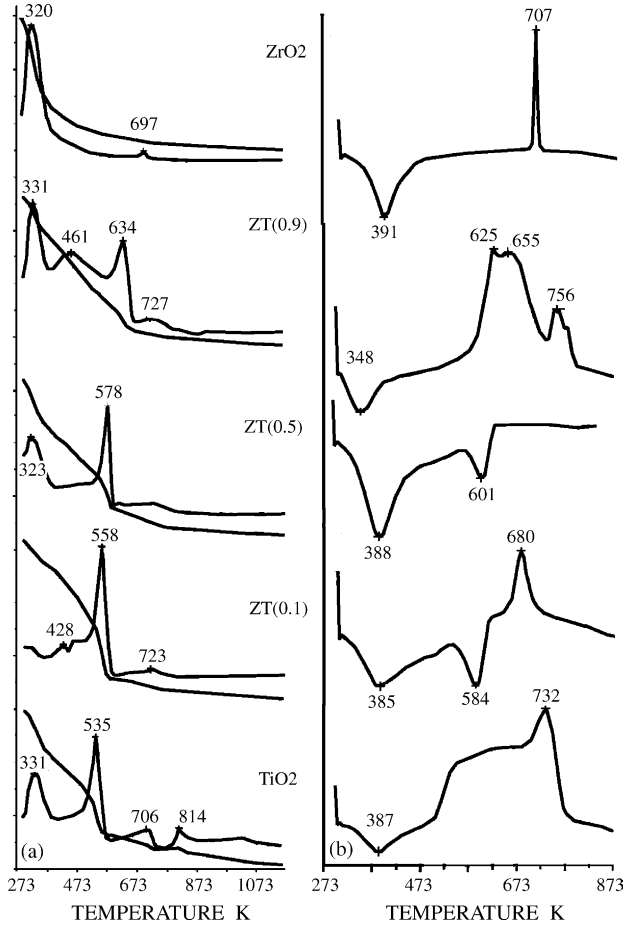

Fig. 1. Thermal analysis of ZrO_2, TiO_2 and ZrO_2–TiO_2 xerogels (a) TGA in the range 293–1073 K and (b) DSC analysis in the range 293–873 K. All measurements were performed under N_2 atmosphere.

Table 1
Surface area (m^2/g)

Supports		Catalysts	
ZrO_2	68	Pt/ZrO_2	42
ZT0.9	225	Pt/ZT(0.9)	181
ZT0.5	552	Pt/ZT(0.5)	465
ZT0.1	241	Pt/ZT(0.1)	177
TiO_2	57	Pt/TiO_2	50

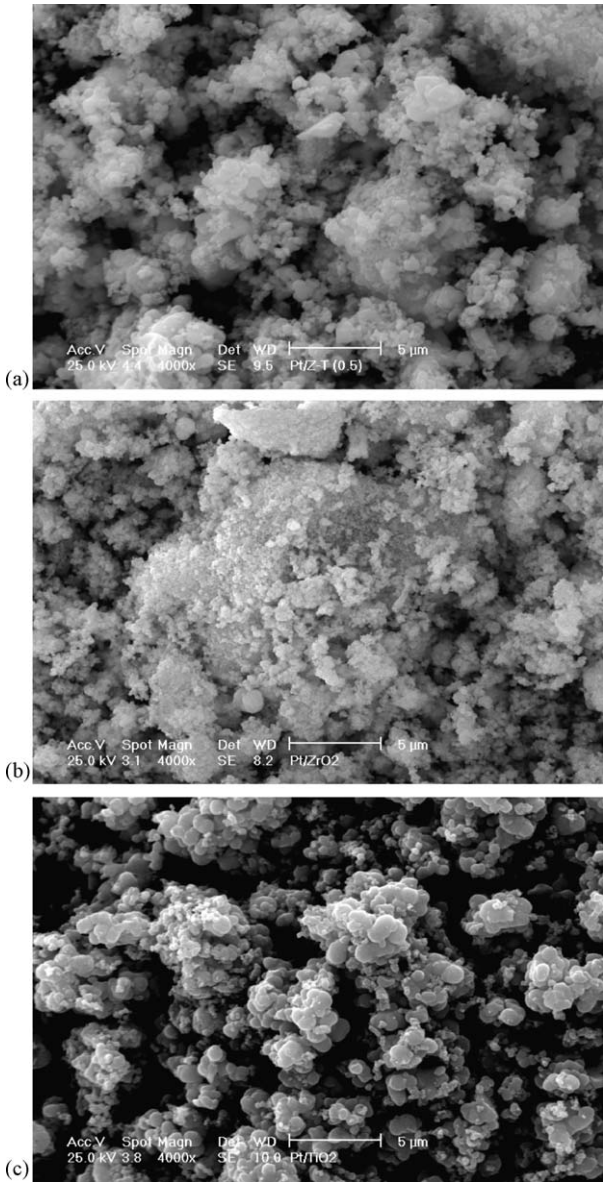

Fig. 2. Typical SEM images of Pt/ZrO_2–TiO_2 catalysts. (a) Pt/ZrO_2, (b) Pt/ZT(0.5) and (c) Pt/TiO_2.

3.3. Crystalline phases

The XRD patterns of the samples are shown in Fig. 3. No evidence of Pt phase was observed in either the pure or the mixed oxide supports. This result is not unexpected considering that the Pt loading in the catalyst is rather low. The Pt/ZrO_2 catalyst showed a mixture of zirconia, tetragonal and monoclinic phases with the former being predominant. In the Pt/TiO_2 sample, the anatase phase of titania was identified. For the binary oxide supports, no peaks attributable to TiO_2 in the Zr-rich oxide, or to ZrO_2 in the Ti-rich oxide, were observed. As a common feature, the intensity of the main peaks in the diffraction pattern decreases and peaks become broader when TiO_2 is incorporated to ZrO_2 or ZrO_2 is incorporated to TiO_2.

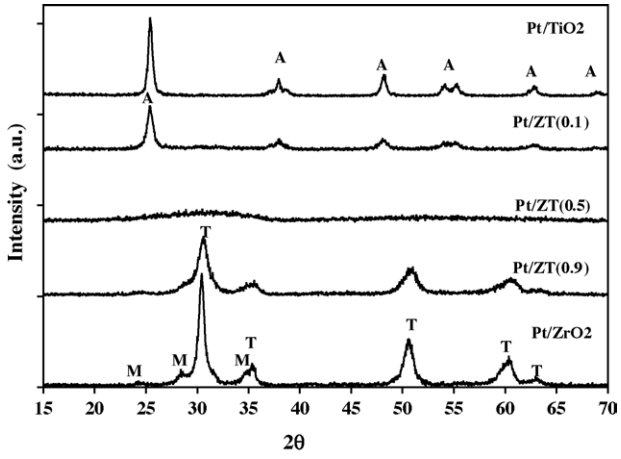

Fig. 3. X-ray diffraction patterns of Pt/ZrO_2–TiO_2 catalysts.

The presence of Ti^{4+} or Zr^{4+} cations in the major oxide structure contributes on one hand to suppression of grain growth and on the other to lattice deformation [18]. Some variations in the cell parameters of the major oxide and a significant diminution of the crystallite size of the major oxide as TiO_2 or ZrO_2 are incorporated (13–9 nm for ZrO_2 and 24–16 nm for TiO_2) were observed. The XRD pattern of the Pt/ZT(0.5) sample presented broad background diffraction lines indicating an amorphous material. This result is in good agreement with the fact that no exothermic events related to a phase transition from an amorphous to a crystalline material were observed in the DSC analysis of the ZT0.5 xerogel sample. Fig. 4 shows HREM images of a Pt particle on the surface of the ZT0.5 support. Pt nanoparticle is about 3.6 nm in diameter with interplanar distance of 0.195 nm assigned to Pt (2 0 0). The amorphous nature of the support is also confirmed by this technique.

3.4. Reduction properties

The TPR profiles of calcined Pt/ZT samples are shown in Fig. 5. Two broad temperature regions where hydrogen is

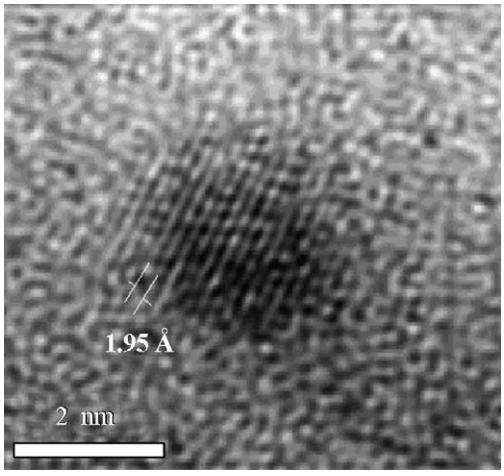

Fig. 4. HREM image of a Pt particle on the ZrO_2–TiO_2(0.5) support.

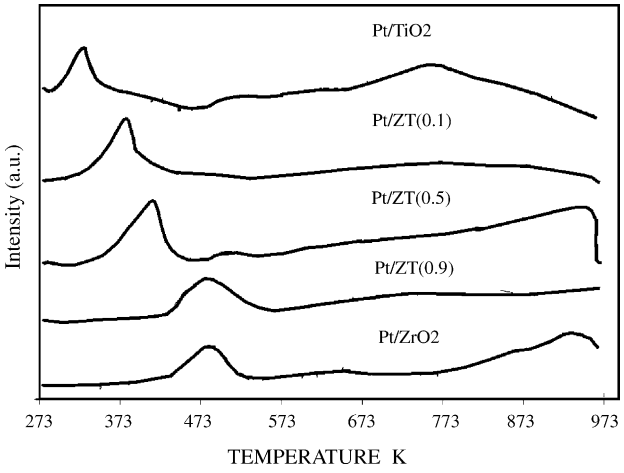

Fig. 5. TPR profiles of calcined Pt/ZrO_2–TiO_2 catalysts.

consumed, roughly below and above 673 K, may be identified. The reduction temperature associated to the peak observed in the first region clearly shifts to lower values as the TiO_2 content in the support increases. This peak is assumed to represent the main reduction of the Pt oxide phase ($Pt^{4+} \rightarrow Pt$). On TiO_2 support, it occurs around 325 K while on ZrO_2 it is observed 490 K. This behavior suggests that the interaction of the Pt oxide phase on each support is different and probably linked to the nature of the surface platinum oxides (chloride-containing and chloride-free) generated from the calcination of the chloroplatinic precursor adsorbed on the support [19,20]. In a previous study [12], XPS showed that the binding energy of the Pt $4f_{7/2}$ level was dependent on the support composition and the reduction pre-treatments performed in situ at 473 and 773 K. Reduction of Pt is achieved at 773 K, although, for Pt supported on ZrO_2 and Zr-rich supports this reduction process is more difficult.

In Table 2 are reported the hydrogen uptakes (theoretical and experimental, the latter related only to the main peak observed below 673 K) and the degree of reduction of the platinum oxide. As observed, from the comparison of the hydrogen uptakes in Table 2, platinum oxide is completely reduced when supported on the ZrO_2–TiO_2 oxides. For Pt/ZrO_2 and Pt/TiO_2 samples the experimental hydrogen uptake is lower compared to the theoretical value. One possible explanation for this result may be that hydrogen consumption associated with small and broad shoulders located after the first peak was not considered. These features could be associated with the reduction of small Pt oxide particles interacting strongly with the support. On the other hand, hydrogen uptakes at temperatures higher than 673 K could be associated with partial reduction of the support. It is well known that reduction of TiO_2 takes place at temperatures higher than 800 K but in the presence of Pt this temperature is lowered [21].

Table 3
Pt dispersion and particle size calculated from H_2 chemisorption experiments

Catalysts	D (%)	ϕ (nm)
Pt/ZrO_2	16	6.2
Pt/ZT(0.9)	15	6.8
Pt/ZT(0.5)	26	3.8
Pt/ZT(0.1)[a]	21	4.9
Pt/TiO_2[a]	17	6.0

[a] Samples reduced at 573 K to avoid SMSI effects.

3.5. Pt particle size and dispersion

Particle size and dispersion of Pt was calculated from H_2 chemisorption measurements and the results are presented in Table 3. TiO_2 and Ti-rich samples were reduced at lower temperature to prevent SMSI effects. Pt particle size and dispersion is about the same when supported on ZrO_2 and Zr-rich support and slightly lower compared to values obtained for Pt when supported on TiO_2 and Ti-rich supports. A better dispersion of Pt is observed for the ZT (0.5) support which presented the highest surface area. Nevertheless, the argument of higher surface area available for Pt dispersion does not explain the result observed in the Pt/ZT(0.9) catalyst, whose surface area was almost five times higher than the one of the ZrO_2 single oxide but Pt dispersion is not improved. Phenomena related to the interaction and mobility of the Pt precursor (oxychloroplatinic PtO_xCl_y species) on the surface of the support during activation process may be taken into account. The slightly higher dispersion of Pt in the Ti-rich supports was also observed by XPS analysis [12].

Table 2
Temperature programmed reduction data of calcined catalysts

Catalyst	Pt (wt.%)[a]	Red. temp. (K)[b]	H_2 uptakes[c] (μmol/g cat)		Reduction extent (%)
			Theoretical	Experimental	
Pt/ZrO_2	1.0	490	102.6	95.8	93.4
Pt/ZT(0.9)	0.92	478	94.6	94.9	100.3
Pt/ZT(0.5)	0.91	413	93.6	97.5	104.2
Pt/ZT(0.1)	0.82	383	84.0	84.0	100
Pt/TiO_2	0.9	332	92.3	83.1	90.0

[a] Determined by EDS.
[b] Reduction temperature (first peak only).
[c] Theoretical and experimental H_2 uptakes assuming $Pt^{4+} \rightarrow Pt$.

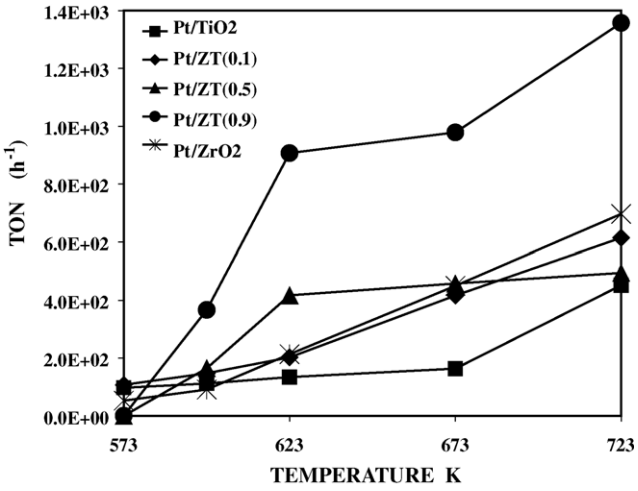

Fig. 6. TON values of Pt/ZrO_2–TiO_2 catalysts in the NO + CH_4 reaction as a function of reaction temperature (NO/CH_4 = 0.5, GHSV = 30500 h^{-1}).

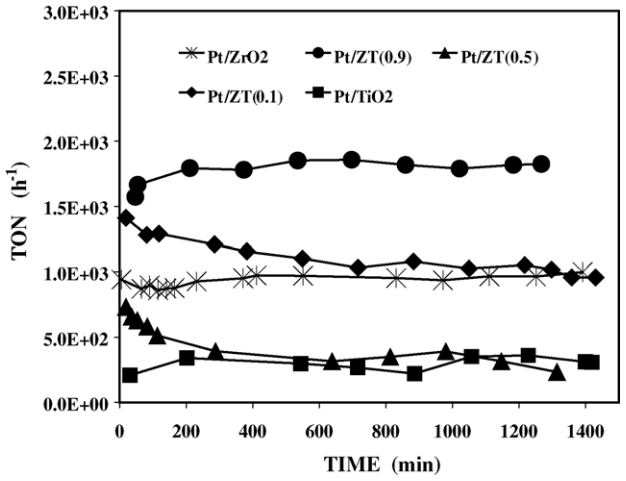

Fig. 8. TON values in the NO + CH_4 reaction as a function of time on stream at 673 K.

3.6. Catalytic activity NO + CH_4 reaction

Any significant catalytic activity of the bare supports was observed (<6% at 773 K). The total activity of the catalysts in terms of the NO conversion measured in the range 573–773 K followed the order: Pt/ZT(0.9) > Pt/ZT(0.5) > Pt/ZrO_2 > Pt/ZT(0.1) > Pt/TiO_2 [22]. Platinum supported on single oxides, presented moderated activity at low temperature but the Pt/ZrO_2 catalyst is more active than the Pt/TiO_2 catalyst in most of the reaction temperature range. The addition of 10 mol% of TiO_2 to the ZrO_2 in the support leads to an improvement of the catalytic activity. All catalysts achieved 100% conversion at 773 K. CH_4 conversion increased as a function of the reaction temperature and it was around 20% for all catalysts at the highest temperature. Only small differences in the behavior of the conversion as a function of the support composition were observed. Fig. 6 shows the calculated TON values for all catalysts as a function of the reaction temperature. The TON value for Pt/ZT(0.9) catalyst is 2.5 times higher compared to that observed for Pt/ZrO_2 catalyst. On the other hand, Pt/ZT(0.1), Pt/ZT(0.5) and Pt/ZrO_2 catalysts have similar TON.

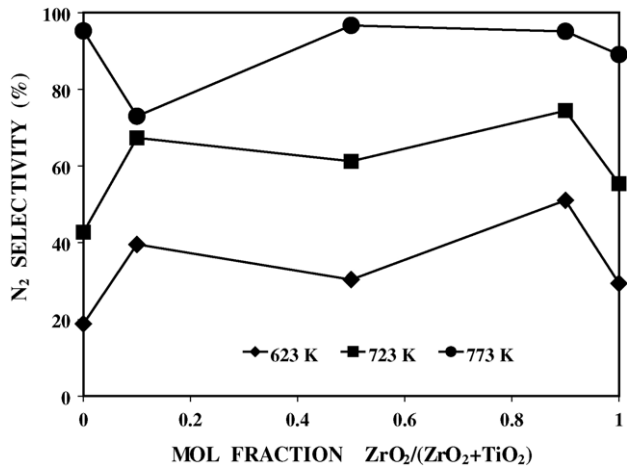

Fig. 7. Evolution of the N_2 selectivity as a function of the support composition. Selectivity was calculated taking into account only nitrogen-containing products (N_2 + N_2O).

The detected reaction products were N_2, N_2O, CO_2 and H_2O. Fig. 7 shows the evolution of the selectivity towards N_2 formation as a function of the support composition at 623, 723 and 773 K. The selectivity was calculated taking into account only nitrogen-containing compounds (N_2 and N_2O). As a general trend the selectivity increases as reaction temperature increases. At 773 K it is almost 100% for Pt/ZrO_2, Pt/TiO_2, Pt/ZT(0.5) and Pt/ZT(0.9) catalysts but a lower selectivity is observed for the Pt/ZT(0.1) catalyst. As a function of the support composition it can be observed that selectivity, on one hand, it is higher for Pt/ZrO_2–TiO_2 catalysts compared to Pt supported on the single oxides and, on the other, that the selectivity is slightly higher on the Pt/ZT(0.9) catalyst.

The stability of the catalysts at 673 K was followed as a function of time on stream. Fig. 8 shows the evolution of TON values for a period of 24 h. Only the Pt/ZT(0.5) catalyst showed some deactivation in that period of time. The Pt/ZT(0.9) as observed is a very active and stable catalyst.

The effect of the addition of N_2O in the feed as a source of oxygen was evaluated. It is well known that oxygen is essential for the reduction of NO with CH_4 [23]. On the other hand, nitrous oxide has been employed as an oxidant for hydrocarbons [24]. Table 4 shows the TON values of Pt/ZrO_2 and Pt/ZT(0.9) catalysts at 673 K before and after addition of 2500 ppm of nitrous oxide to the reaction

Table 4
Comparison of TON (h^{-1}) values at 673 K in absence and presence of N_2O

Catalyst	NO + CH_4	NO + CH_4 + N_2O
Pt/ZrO_2	450	761
Pt/ZT(0.9)	979	1250

mixture. As observed the TON increases in the presence of N_2O. Li and Armor [25] studied the effect of N_2O in the catalytic behavior of Co-ZSM-5 for the NO + CH_4 reaction. They have shown that the addition of N_2O in the feed increased the activity of the catalyst in the absence of O_2.

Mixed oxides often show enhanced acidity in comparison to the respective single oxide components. It is well known that ZrO_2–TiO_2 exhibits high surface acidity by a charge imbalance based on the generation of Ti–O–Zr bonding according to Tanabe model [26]. The model predicts Lewis acidity in the Zr-rich binary oxide, while in the Ti-rich binary oxide, Brönsted acidity is expected. In line with this Lahousse et al. [27] reported for the ZrO_2 (23%)–TiO_2 (77%) binary oxide the existence of Brönsted acidity. On the other hand, it is considered that acid sites play an important role for the SCR of NO by hydrocarbons. Some reports have shown that the role of acid sites is to promote the NO oxidation steps [4–7]. In a previous work surface properties of the Pt/ZrO_2–TiO_2 catalysts were investigated [12]. IR spectroscopy in its DRIFT mode was used to study the surface species generated as the catalysts were exposed to an NO + O_2 gas mixture. The 1800–1100 cm^{-1} range was examined and the observed peaks were assigned to nitrite/nitrate species. The appearance of such species (NO_x^-, $x = 2, 3$) which are formed on Lewis acid sites [28] was used as an indirect characterization of the catalyst acidity. It was shown that all Zr-containing catalysts developed these nitrite/nitrate species on the surface. In the same work [12], DRIFT spectra of Pt/ZrO_2, Pt/ZT(0.9) and Pt/ZT(0.5) catalysts under NO + CH_4 reaction in the absence of oxygen were recorded at different temperatures. Only the Pt/ZT(0.9) catalyst showed the presence of a moderately intense band at 2037 cm^{-1} and a less intense one at 2206 cm^{-1}. The band at 2037 cm^{-1} was associated with isocyano (−NC) species and the band at 2206 cm^{-1} was assigned to isocyanate species (−NCO) [29]. The isocyanate species were assumed to be produced by oxidation of the isocyano species by the water produced in the reaction since no oxygen was fed into the system.

Although the acidic properties of the catalyst surface and the formation of stable isocyano species at high temperature in Zr-rich catalysts at the Pt-support interface and in particular in the Pt/ZT(0.9) catalyst could explain the reactivity of this catalyst, particle size effects may also be examined. It is known that the SCR-HC is a structure sensitive reaction [30–33]. Demicheli et al. [32] have shown for the NO reduction by CH_4 the influence of metal particle size on the activity and selectivity of Pt and Pt–Au/Al_2O_3 catalysts. They found that the specific reaction rate increased with increasing particle size from 1.5 to 15 nm indicating that the reaction can occur preferentially on large Pt planes. Balint et al. [31] have shown for the NO/CH_4 reaction that both, the size and the dominant crystallographic orientation of Pt supported particles are determining factors for the catalyst activity and selectivity. In this view, the Pt/ZT(0.9) catalyst which presented the largest particle size is also the most active.

4. Conclusions

The catalytic performance for the selective reduction of NO by CH_4 of Pt supported on ZrO_2–TiO_2 binary oxide prepared by sol–gel was investigated. ZrO_2–TiO_2 mixed oxides with various $ZrO_2/ZrO_2 + TiO_2$ composition (0.9, 0.5 and 0.1) were prepared by the sol–gel method. For supports calcined at 773 K as a function of the support composition the surface area of the ZrO_2–TiO_2 oxides goes through a maximum (552 m^2/g) for the (ZT0.5) support whose surface area was almost nine times higher than the one of the single oxides (around 60 m^2/g). XRD spectra showed for Zr-rich supports a mixture of tetragonal and monoclinic phases of ZrO_2 with the former being predominant. For TiO_2 and Ti-rich oxides anatase was the predominant crystalline phase. The ZT0.5 support was almost amorphous. On the other hand, Pt oxide reduction temperature was also dependent on the support composition. The reduction temperature decreases as TiO_2 is added to the support. The steady-state activity of the catalysts was also dependent on the support composition. The reactivity of the catalysts (TON) in the range 573–773 K follows the order: Pt/ZT(0.9) > Pt/ZrO_2 ≈ Pt/ZT(0.5) ≈ Pt/ZT(0.1) > Pt/TiO_2. The Pt/ZT(0.9) catalyst showed the highest catalytic activity with TON values as 2.5 times higher compared to Pt/ZrO_2. Also, the selectivity for N_2 production was slightly higher for this catalyst. Pt particle size for this catalyst was the largest. All catalysts improved their performance in the presence of N_2O. The combination of acid properties, particle size and the presence of stable isocyano type intermediates at the Pt-support interface which characterize the Pt/ZT(0.9) catalyst may explain its performance.

Acknowledgements

This research was supported partially by CONACYT (27647U). Technical help from Samuel Tehuacanero (Image processing), Manuel Aguilar (XRD) and Luis Rendón (HRTEM) is also acknowledged.

References

[1] H. Bosh, F.J.J.G. Janssen, Catal. Today 2 (1998) 369.
[2] M. Shelef, Chem. Rev. 95 (1995) 209.
[3] Y. Nishizaka, M. Misono, Chem. Lett. (No. 8) (1993) 1295.
[4] Y. Li, J.N. Armor, J. Catal. 145 (1994) 393.
[5] J.O. Petunchi, W.K. Hall, Appl. Catal. B 2 (1993) L17.
[6] T. Miller, E. Glusker, R. Peddi, T. Zheng, J.R. Regalbuto, Catal. Lett. 51 (1998) 15.
[7] C.J. Loughran, D.E. Resasco, Appl. Catal. B 7 (1995) 113.
[8] H. Hosose, H. Yahiro, N. Mizuno, M. Iwamoto, Chem. Lett. (No. 10) (1991) 1859.
[9] M. Haneda, Y. Kintaichi, M. Inaba, H. Hamada, Bull. Chem. Soc. Jpn. 70 (1997) 499.
[10] E.P. Reddy, T.C. Rojas, A. Fernández, Langmuir 16 (2002) 4217.
[11] C.-M. Lu, Y.-M. Lin, I. Wang, Appl. Catal. A 198 (2000) 223.

[12] R. Mariscal, S. Rojas, A. Gómez-Cortés, G. Díaz, R. Pérez, J.L.G. Fierro, Catal. Today 75 (2002) 385.
[13] J. Rodriguez-Carvajal, Physica B 192 (1993) 55.
[14] I.A. Montoya, T. Viveros, J.M. Domínguez, L.A. Canales, I. Schifter, Catal. Lett. 15 (1992) 207.
[15] A. Knell, P. Barnickeñ, A. Baiker, A. Wokaun, J. Catal. 137 (1992) 306.
[16] H. Xie, Q. Zhang, T. Xi, J. Wang, Y. Liu, Thermochimica Acta. 381 (2002) 45–48.
[17] Q. Xu, M. Anderson, J. Am. Ceram. Soc. 76 (1993) 2093.
[18] Y.M. Wang, S.W. Liu, M.K. Lü, Sh.F. Wang, F. Gu, X.Zh. Gai, X.P. Cui, J. Pan, J. Mol. Catal. A: Chemical 215 (2004) 137.
[19] H. Lieske, G. Lietz, H. Spindler, J. Völter, J. Catal. 81 (1983) 8.
[20] G. Lietz, H. Spindler, H. Lieske, W. Hanke, J. Völter, J. Catal. 81 (1983) 17.
[21] B.A. Sexton, A.E. Hughes, K. Foger, J. Catal. 77 (1982) 85.
[22] R. Pérez-Hernández, A. Gómez-Cortés, J. Arenas-Alatorre, R. Mariscal, J.L.G. Fierro, G. Díaz, Proc. XIX Iberoamerican Catalysis Symposium, Mérida Yucatán, 5–10 September, 2004, p. 117.
[23] R. Burch, J.P. Breen, F.C. Meunier, Appl. Catal. B 39 (2002) 283.
[24] H.-F. Liu, R.-S. Liu, K.Y. Liew, R.E. Johnson, J.H. Lunsford, J. Am. Chem. Soc. 106 (1984) 4117.
[25] Y. Li, J.N. Armor, Appl. Catal. B 3 (1993) 55.
[26] K. Tanabe, T. Sumiyoshi, K. Shibata, T. Kiyoura, J. Kitagawa, Bull. Chem. Soc. Jpn. 47 (5) (1974) 1064.
[27] C. Lahousse, A. Aboulayt, F. Maugé, J. Bachelier, J.C. Lavalley, J. Mol. Catal. 84 (1993) 283.
[28] K.I. Hadjiivanov, Catal. Rev. Sci. Eng. 42 (2000) 71.
[29] F. Poignant, J. Saussey, J.-C. Lavalley, G. Mabilon, Catal. Today 29 (1996) 93.
[30] B.C. Gates, Chem. Rev. 95 (1995) 511.
[31] I. Balint, A. Miyazaki, K.-I. Aika, Appl. Catal. B 37 (2002) 217.
[32] M.C. Demicheli, L.C. Hoang, J.C. Ménézo, J. Barbier, M. Oinabiau-Carlier, Appl. Catal. A 97 (1993) L11.
[33] R. Burch, A. Ramli, Appl. Catal. B 15 (1998) 49.